

Supplement of Atmos. Chem. Phys., 20, 1255–1276, 2020
<https://doi.org/10.5194/acp-20-1255-2020-supplement>
© Author(s) 2020. This work is distributed under
the Creative Commons Attribution 4.0 License.



Atmospheric
Chemistry
and Physics
Open Access

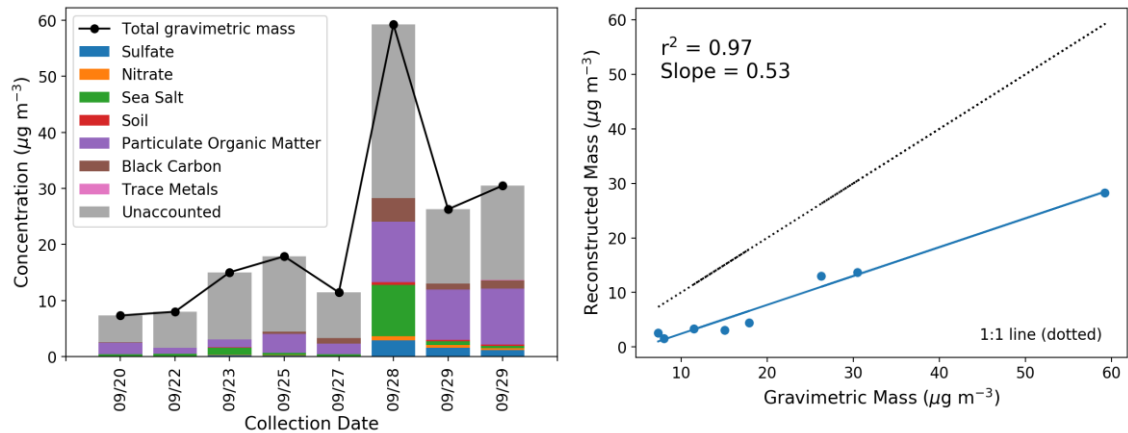

Supplement of

Investigating size-segregated sources of elemental composition of particulate matter in the South China Sea during the 2011 *Vasco* cruise

Miguel Ricardo A. Hilario et al.

Correspondence to: Maria Obiminda L. Cambaliza (mcambaliza@ateneo.edu)

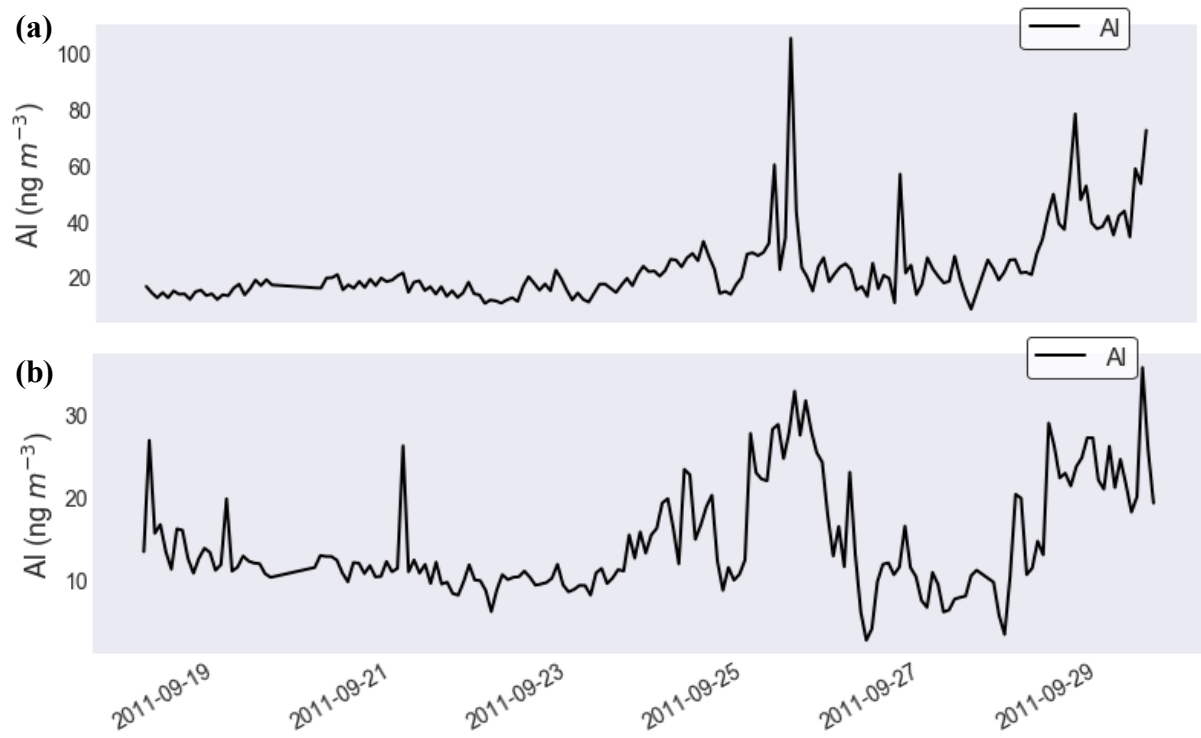
The copyright of individual parts of the supplement might differ from the CC BY 4.0 License.



20

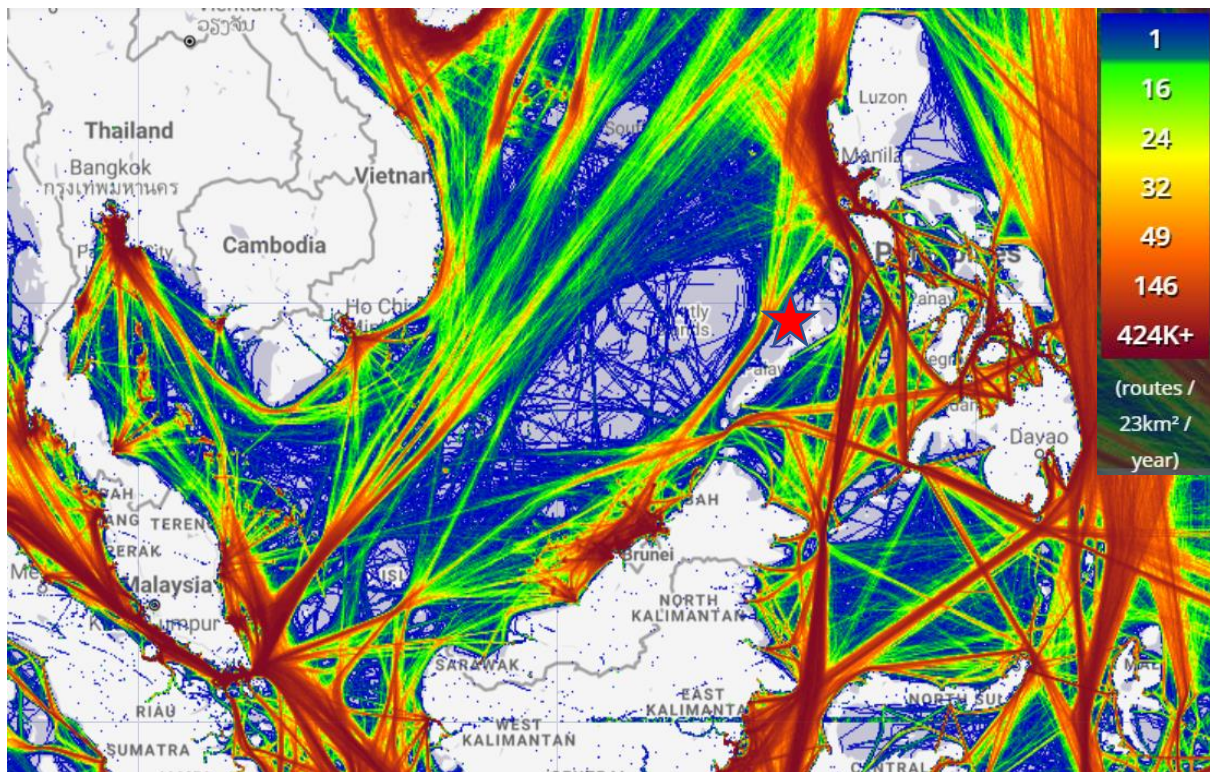
21 **Figure S1. (a) Contributions of PM_{2.5} components ($\mu\text{g m}^{-3}$) derived from filters collected**
 22 **during the cruise. (b) Linear regression (blue) of gravimetric and reconstructed masses**
 23 **($\mu\text{g m}^{-3}$) with a 1-to-1 line depicted as a dashed line (black). Methodology for the mass**
 24 **reconstruction is found in Malm and Hand (2007).**

25



26

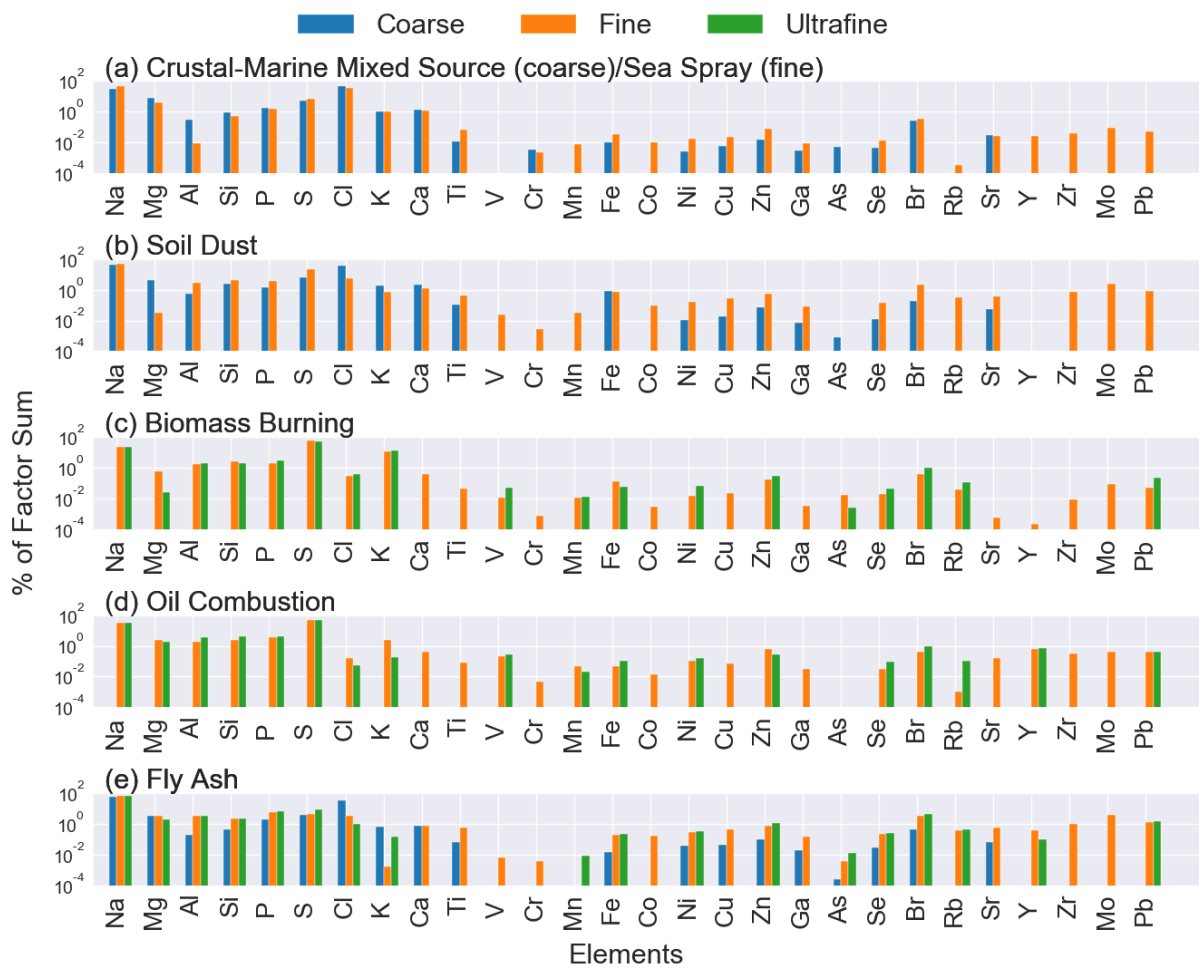
27 **Figure S2.** Time series of Al in the (a) fine and (b) ultrafine modes.



28

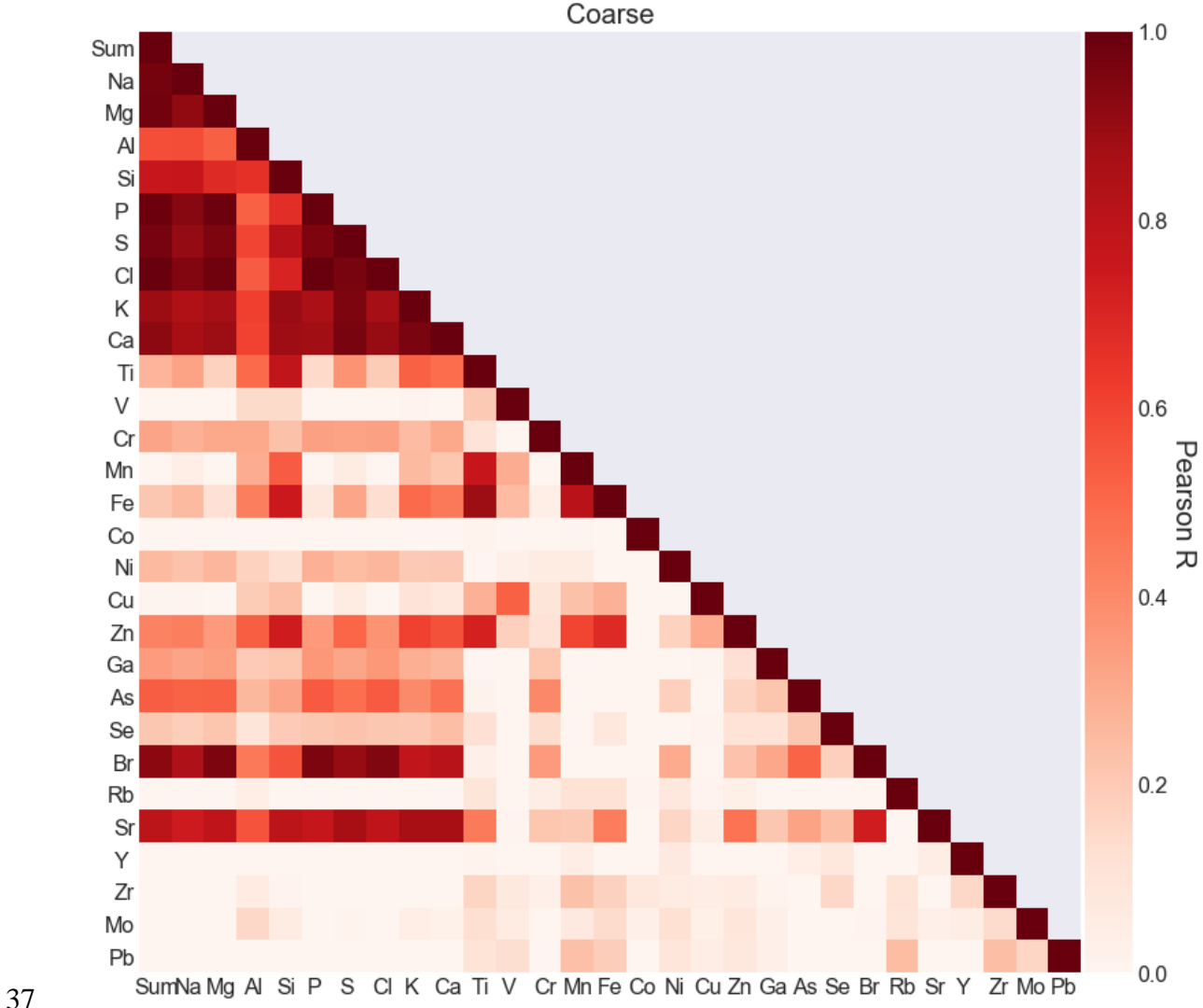
29 **Figure S3. Ship tracks near the Palawan sampling site for 2016-2017. Red star indicates**
30 **the location of the M/Y Vasco. Source: MarineTraffic.**

31



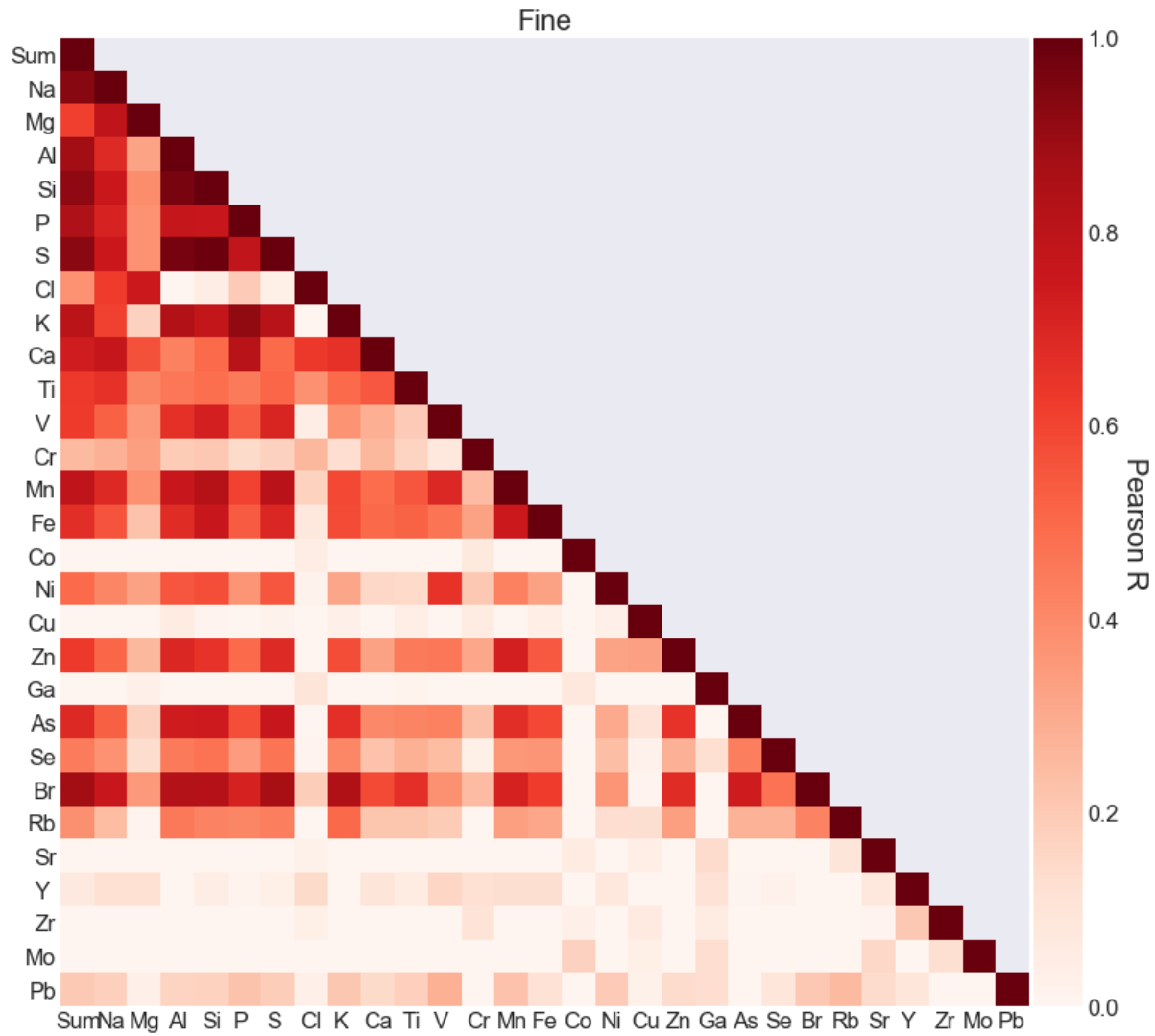
32

33 **Figure S4. PMF source profiles across different size ranges displayed by percent of**
 34 **factor sum for (a) sea spray, (b) soil dust, (c) biomass burning, (d) oil combustion, and**
 35 **(e) fly ash. Coarse: Stage 1-3 ($1.15\text{-}10 \mu\text{m}$; blue), Fine: Stage 4-6 ($0.34\text{-}1.15 \mu\text{m}$; orange),**
 36 **Ultrafine: Stage 7-8 ($0.10\text{-}0.34 \mu\text{m}$; green).**



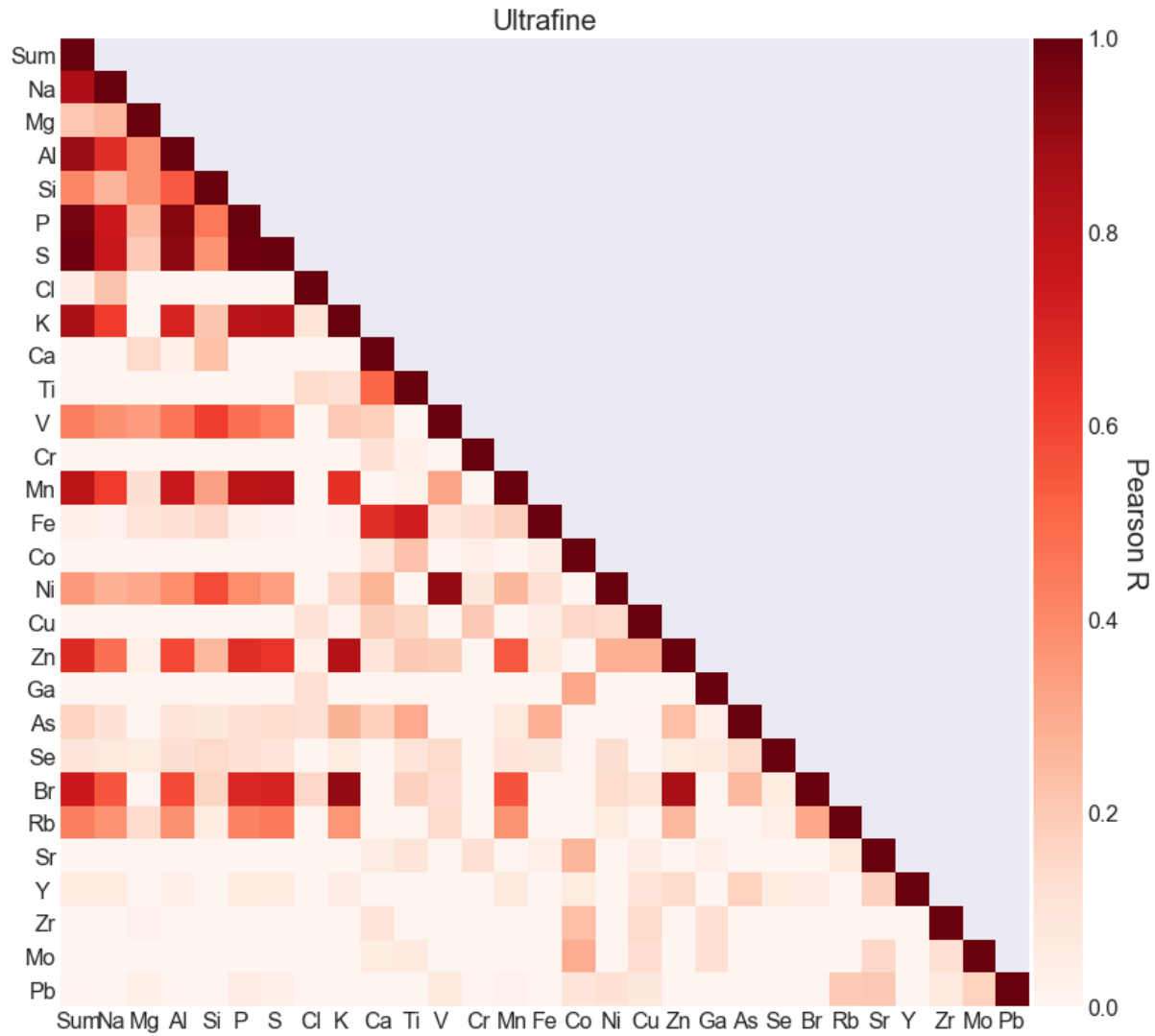
37

38 **Figure S5. Correlation heatmap for the coarse mode (1.15 – 10 μm).**



39

40 **Figure S6. Correlation heatmap for the fine mode (0.34 – 1.15 μm).**



41

42 **Figure S7. Correlation heatmap for the ultrafine mode (0.07-0.34 μm).**

Table S1. Pearson correlation matrix for the coarse mode (1.15 - 10 µm). Correlation coefficients above 0.7 are marked in bold.

	Sum	Na	Mg	Al	Si	P	S	Cl	K	Ca	Ti	V	Cr	Mn	Fe	Co	Ni	Cu	Zn	Ga	As	Se	Br	Rb	Sr	Y	Zr	Mo	Pb
Sum	1.00																												
Na	0.97	1.00																											
Mg	0.97	0.91	1.00																										
Al	0.57	0.58	0.53	1.00																									
Si	0.76	0.76	0.68	0.66	1.00																								
P	0.99	0.93	0.98	0.52	0.67	1.00																							
S	0.97	0.91	0.95	0.60	0.82	0.95	1.00																						
Cl	0.99	0.94	0.98	0.54	0.70	1.00	0.96	1.00																					
K	0.89	0.84	0.87	0.61	0.90	0.85	0.95	0.87	1.00																				
Ca	0.92	0.87	0.89	0.60	0.88	0.88	0.96	0.90	0.96	1.00																			
Ti	0.27	0.32	0.17	0.50	0.78	0.15	0.37	0.19	0.52	0.49	1.00																		
V	-0.11	-0.10	-0.13	0.14	0.14	-0.15	-0.05	-0.13	0.01	0.00	0.20	1.00																	
Cr	0.32	0.28	0.31	0.31	0.23	0.33	0.32	0.33	0.25	0.31	0.10	-0.06	1.00																
Mn	-0.03	0.04	-0.13	0.29	0.54	-0.15	0.06	-0.11	0.25	0.21	0.76	0.29	-0.08	1.00															
Fe	0.21	0.25	0.11	0.43	0.75	0.08	0.31	0.13	0.50	0.45	0.89	0.25	0.04	0.81	1.00														
Co	-0.07	-0.04	-0.09	-0.06	-0.06	-0.09	-0.09	-0.08	-0.10	-0.09	0.01	-0.04	-0.08	0.00	-0.02	1.00													
Ni	0.25	0.22	0.26	0.17	0.12	0.28	0.25	0.26	0.20	0.21	-0.02	0.03	0.06	0.06	-0.05	-0.03	1.00												
Cu	0.01	0.01	-0.02	0.19	0.23	-0.02	0.05	-0.01	0.10	0.08	0.28	0.52	0.09	0.23	0.28	-0.02	-0.02	1.00											
Zn	0.42	0.44	0.35	0.53	0.74	0.35	0.51	0.37	0.61	0.56	0.72	0.18	0.11	0.60	0.68	-0.03	0.17	0.30	1.00										
Ga	0.35	0.32	0.34	0.20	0.21	0.36	0.31	0.36	0.29	0.26	0.00	-0.04	0.21	-0.06	0.00	-0.05	-0.06	0.00	0.12	1.00									
As	0.53	0.52	0.52	0.26	0.32	0.54	0.48	0.54	0.40	0.47	0.02	-0.13	0.40	-0.09	-0.02	-0.05	0.18	-0.02	0.16	0.22	1.00								
Se	0.21	0.19	0.22	0.09	0.20	0.21	0.22	0.21	0.21	0.24	0.12	-0.07	0.14	-0.01	0.08	-0.07	-0.10	0.01	0.11	0.11	0.21	1.00							
Br	0.92	0.84	0.95	0.45	0.56	0.95	0.90	0.95	0.78	0.82	0.03	-0.18	0.35	-0.26	-0.02	-0.09	0.30	-0.06	0.23	0.31	0.51	0.18	1.00						
Rb	-0.17	-0.15	-0.21	0.04	-0.03	-0.18	-0.15	-0.18	-0.11	-0.13	0.10	-0.02	0.05	0.11	0.11	0.01	0.08	0.01	0.04	-0.09	-0.11	-0.02	-0.19	1.00					
Sr	0.80	0.74	0.79	0.56	0.80	0.77	0.87	0.79	0.86	0.86	0.45	0.01	0.21	0.20	0.44	-0.09	0.16	0.05	0.47	0.21	0.32	0.24	0.73	-0.11	1.00				
Y	-0.09	-0.09	-0.08	-0.07	-0.05	-0.08	-0.05	-0.09	-0.06	-0.04	0.01	-0.16	-0.02	0.04	-0.01	-0.09	0.07	-0.10	-0.05	-0.08	0.04	0.08	-0.07	-0.14	0.05	1.00			
Zr	-0.15	-0.10	-0.20	0.05	0.01	-0.18	-0.17	-0.17	-0.11	-0.13	0.16	0.07	0.03	0.23	0.17	0.08	0.05	0.05	0.05	0.01	-0.10	0.16	-0.18	0.11	-0.13	0.15	1.00		
Mo	-0.02	-0.03	-0.01	0.15	0.06	-0.03	0.01	-0.03	0.04	0.03	0.12	0.06	-0.04	0.07	0.14	0.03	0.12	0.04	0.09	0.03	-0.11	-0.03	0.01	0.10	0.03	0.04	0.14	1.00	
Pb	-0.33	-0.32	-0.35	-0.01	-0.13	-0.34	-0.30	-0.34	-0.23	-0.28	0.10	0.13	-0.08	0.23	0.19	-0.09	0.09	0.05	0.08	0.03	-0.48	-0.26	-0.34	0.24	-0.13	-0.02	0.24	0.16	1.00

Table S2. Pearson correlation matrix for the fine mode (0.34 – 1.15 µm). Correlation coefficients above 0.7 are marked in bold.

	Sum	Na	Mg	Al	Si	P	S	Cl	K	Ca	Ti	V	Cr	Mn	Fe	Co	Ni	Cu	Zn	Ga	As	Se	Br	Rb	Sr	Y	Zr	Mo	Pb
Sum	1.00																												
Na	0.93	1.00																											
Mg	0.61	0.79	1.00																										
Al	0.88	0.68	0.32	1.00																									
Si	0.92	0.75	0.39	0.96	1.00																								
P	0.84	0.71	0.37	0.77	0.76	1.00																							
S	0.93	0.75	0.37	0.97	0.98	0.78	1.00																						
Cl	0.37	0.62	0.75	-0.08	0.05	0.20	0.04	1.00																					
K	0.80	0.61	0.17	0.83	0.78	0.91	0.81	-0.02	1.00																				
Ca	0.73	0.77	0.57	0.43	0.49	0.81	0.49	0.63	0.66	1.00																			
Ti	0.63	0.66	0.41	0.46	0.48	0.45	0.51	0.38	0.50	0.55	1.00																		
V	0.63	0.52	0.35	0.66	0.72	0.53	0.70	0.05	0.37	0.29	0.20	1.00																	
Cr	0.25	0.28	0.33	0.19	0.21	0.14	0.18	0.26	0.13	0.26	0.17	0.07	1.00																
Mn	0.79	0.69	0.38	0.76	0.82	0.60	0.81	0.17	0.59	0.49	0.55	0.69	0.25	1.00															
Fe	0.67	0.56	0.22	0.68	0.76	0.54	0.69	0.08	0.58	0.50	0.52	0.47	0.32	0.75	1.00														
Co	-0.43	-0.34	-0.12	-0.44	-0.47	-0.42	-0.47	0.04	-0.40	-0.29	-0.20	-0.42	0.07	-0.43	-0.45	1.00													
Ni	0.49	0.41	0.33	0.55	0.57	0.37	0.55	0.02	0.32	0.15	0.15	0.65	0.20	0.43	0.33	-0.20	1.00												
Cu	-0.04	-0.09	-0.13	0.06	0.01	-0.02	0.02	-0.19	0.03	-0.10	0.04	-0.01	0.06	-0.07	0.04	0.00	0.03	1.00											
Zn	0.63	0.50	0.26	0.69	0.66	0.49	0.68	0.00	0.58	0.33	0.45	0.46	0.31	0.72	0.55	-0.36	0.32	0.33	1.00										
Ga	-0.11	-0.05	0.03	-0.15	-0.17	-0.13	-0.15	0.09	-0.15	-0.10	0.02	-0.09	-0.07	-0.12	-0.18	0.08	-0.01	-0.06	-0.04	1.00									
As	0.69	0.53	0.17	0.73	0.74	0.57	0.76	-0.03	0.67	0.40	0.42	0.43	0.23	0.67	0.59	-0.33	0.30	0.10	0.66	-0.23	1.00								
Se	0.44	0.37	0.13	0.45	0.47	0.35	0.47	0.01	0.41	0.22	0.28	0.24	0.04	0.36	0.36	-0.17	0.23	0.02	0.28	0.12	0.43	1.00							
Br	0.88	0.76	0.35	0.83	0.82	0.71	0.86	0.19	0.84	0.58	0.67	0.38	0.25	0.71	0.62	-0.32	0.36	0.01	0.68	-0.10	0.74	0.47	1.00						
Rb	0.38	0.24	0.01	0.45	0.42	0.41	0.44	-0.13	0.50	0.22	0.22	0.19	-0.01	0.33	0.31	-0.15	0.13	0.13	0.34	-0.13	0.28	0.28	0.42	1.00					
Sr	-0.18	-0.14	-0.08	-0.17	-0.19	-0.21	-0.19	0.03	-0.21	-0.14	-0.06	-0.05	-0.10	-0.10	-0.11	0.06	-0.03	0.04	-0.04	0.14	-0.21	-0.01	-0.16	0.09	1.00				
Y	0.07	0.12	0.12	-0.01	0.04	0.01	0.04	0.14	-0.07	0.09	0.06	0.16	0.12	0.13	0.13	-0.10	0.08	-0.14	-0.04	0.11	0.01	0.02	-0.02	-0.22	0.08	1.00			
Zr	-0.13	-0.12	-0.01	-0.14	-0.13	-0.08	-0.15	0.04	-0.14	-0.03	-0.04	-0.05	0.10	-0.08	-0.01	0.03	-0.02	0.06	-0.06	0.06	-0.13	-0.02	-0.18	-0.11	0.01	0.21	1.00		
Mo	-0.27	-0.27	-0.21	-0.17	-0.23	-0.20	-0.22	-0.21	-0.19	-0.27	-0.11	-0.13	-0.22	-0.19	-0.23	0.17	-0.03	0.04	-0.16	0.13	-0.21	-0.16	-0.23	-0.07	0.15	-0.02	0.12	1.00	
Pb	0.20	0.18	0.03	0.17	0.17	0.22	0.19	0.03	0.21	0.14	0.18	0.28	-0.03	0.23	0.11	-0.14	0.20	0.03	0.14	0.13	-0.07	0.09	0.20	0.25	0.14	0.09	-0.11	-0.01	1.00

Table S3. Pearson correlation matrix for the ultrafine mode (0.07-0.34 µm). Correlation coefficients above 0.7 are marked in bold.

	Sum	Na	Mg	Al	Si	P	S	Cl	K	Ca	Ti	V	Cr	Mn	Fe	Co	Ni	Cu	Zn	Ga	As	Se	Br	Rb	Sr	Y	Zr	Mo	Pb
Sum	1																												
Na	0.85	1																											
Mg	0.21	0.25	1																										
Al	0.9	0.68	0.38	1																									
Si	0.4	0.27	0.38	0.54	1																								
P	0.97	0.75	0.26	0.94	0.45	1																							
S	0.98	0.77	0.2	0.91	0.37	0.98	1																						
Cl	0.05	0.22	-0.29	-0.3	-0.15	-0.1	-0.06	1																					
K	0.86	0.63	-0.01	0.71	0.22	0.81	0.83	0.1	1																				
Ca	-0.04	-0.04	0.15	0.03	0.23	-0.01	-0.07	-0.02	-0.05	1																			
Ti	-0.02	-0.04	-0.1	-0.04	0	-0.04	-0.06	0.14	0.12	0.51	1																		
V	0.44	0.38	0.34	0.47	0.62	0.48	0.43	-0.07	0.2	0.18	-0.09	1																	
Cr	-0.11	-0.11	-0.03	-0.09	-0.06	-0.12	-0.1	-0.05	-0.11	0.11	0.03	-0.06	1																
Mn	0.8	0.63	0.12	0.76	0.33	0.8	0.81	-0.04	0.66	-0.02	0.03	0.32	-0.03	1															
Fe	0.04	0.02	0.09	0.11	0.16	0.04	0.02	-0.02	0.02	0.67	0.73	0.09	0.13	0.17	1														
Co	-0.62	-0.53	-0.12	-0.55	-0.21	-0.59	-0.62	-0.06	-0.51	0.1	0.22	-0.34	0.03	-0.51	0.04	1													
Ni	0.35	0.28	0.31	0.39	0.58	0.39	0.33	-0.07	0.15	0.27	-0.04	0.91	0.08	0.26	0.11	-0.25	1												
Cu	-0.09	-0.09	-0.19	-0.14	-0.16	-0.11	-0.11	0.11	0.02	0.19	0.16	-0.16	0.2	-0.02	0.05	0.15	0.14	1											
Zn	0.68	0.48	0.04	0.59	0.25	0.67	0.64	0.03	0.82	0.09	0.2	0.19	-0.01	0.54	0.07	-0.32	0.28	0.28	1										
Ga	-0.23	-0.15	-0.08	-0.29	-0.2	-0.25	-0.25	0.11	-0.16	-0.19	-0.06	-0.12	-0.08	-0.24	-0.23	0.31	-0.13	-0.04	-0.17	1									
As	0.17	0.11	-0.04	0.1	0.08	0.12	0.13	0.12	0.28	0.18	0.3	-0.01	-0.03	0.07	0.28	-0.05	-0.02	0.01	0.23	0.03	1								
Se	0.09	0.07	0.06	0.12	0.14	0.11	0.09	-0.06	0.05	-0.01	0.1	0.14	-0.04	0.1	0.08	0.01	0.13	-0.11	0.05	0.07	0.14	1							
Br	0.75	0.55	-0.1	0.58	0.16	0.69	0.71	0.16	0.91	-0.03	0.17	0.13	-0.07	0.56	-0.01	-0.38	0.13	0.1	0.86	-0.08	0.26	0.05	1						
Rb	0.44	0.37	0.14	0.38	0.05	0.42	0.45	-0.09	0.36	-0.16	-0.1	0.14	-0.03	0.37	-0.13	-0.24	0.06	-0.08	0.26	-0.04	-0.09	0.04	0.31	1					
Sr	-0.21	-0.14	-0.04	-0.19	-0.12	-0.2	-0.21	0	-0.22	0.05	0.09	-0.16	0.11	-0.2	0.03	0.26	-0.14	0.05	-0.16	0.03	-0.11	-0.07	-0.17	0.07	1				
Y	0.06	0.06	-0.12	0.03	0	0.05	0.06	0	0.05	-0.13	-0.07	-0.09	-0.07	0.07	-0.08	0.06	-0.07	0.09	0.14	-0.06	0.17	0.05	0.05	-0.18	0.17	1			
Zr	-0.33	-0.28	0.02	-0.29	-0.14	-0.32	-0.33	0.01	-0.26	0.1	-0.01	-0.15	0	-0.33	-0.12	0.24	-0.06	0.15	-0.16	0.12	-0.12	0	-0.22	-0.19	0	-0.02	1		
Mo	-0.27	-0.26	-0.08	-0.25	-0.07	-0.26	-0.28	-0.01	-0.2	0.06	0.07	-0.14	-0.02	-0.25	-0.01	0.29	-0.08	0.13	-0.04	0.12	-0.04	-0.13	-0.08	-0.04	0.16	-0.07	0.12	1	
Pb	0.01	-0.04	0.04	0.01	-0.01	0.05	0.03	-0.03	-0.05	-0.06	-0.14	0.06	0.01	0.02	-0.18	0.09	0.11	0.08	-0.01	0	-0.53	-0.08	0.01	0.19	0.21	-0.1	0.07	0.17	1

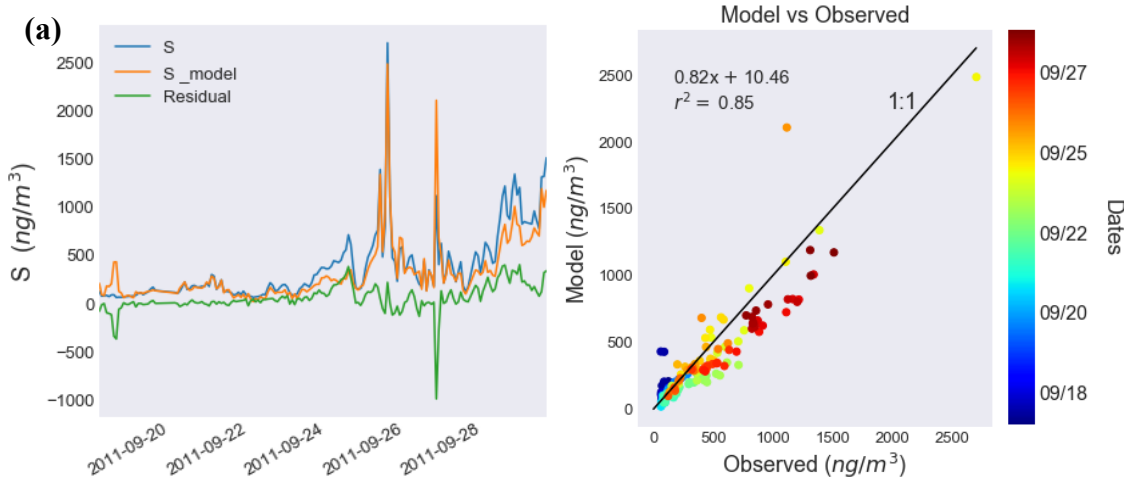
48 **Table S4. Comparison of ratio-slopes and r² correlations of various elements with stage**

49 **7-8 Si.**

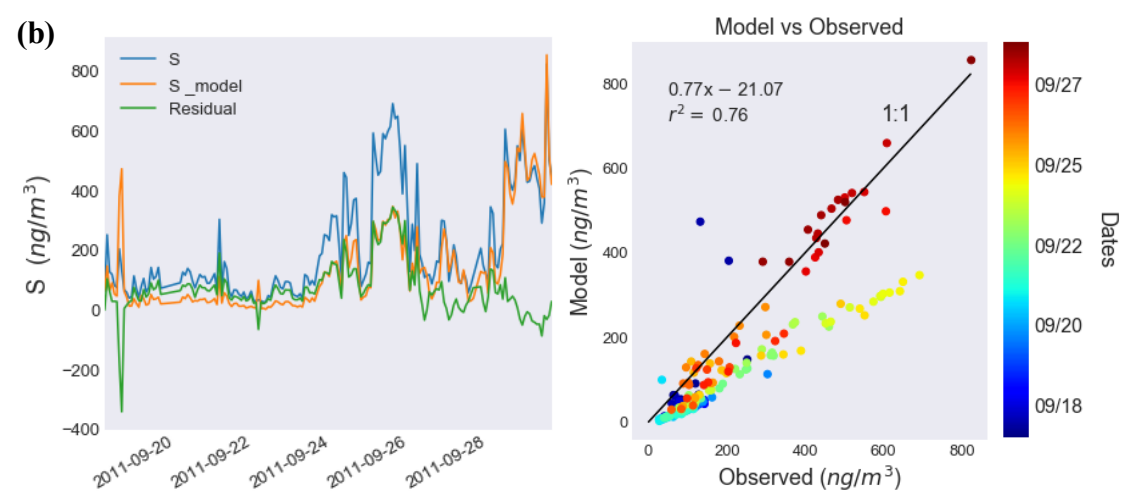
	18-19 Sept			19-30 Sept		
	Ratio-slope	R ²	Intercept	Ratio-slope	R ²	Intercept
P	0.06	0.76	16.36	0.83	0.96	10.45
S	1.73	0.73	11.67	22.26	0.94	-84.65
Al	0.11	0.61	9.4	0.81	0.92	3.47

50

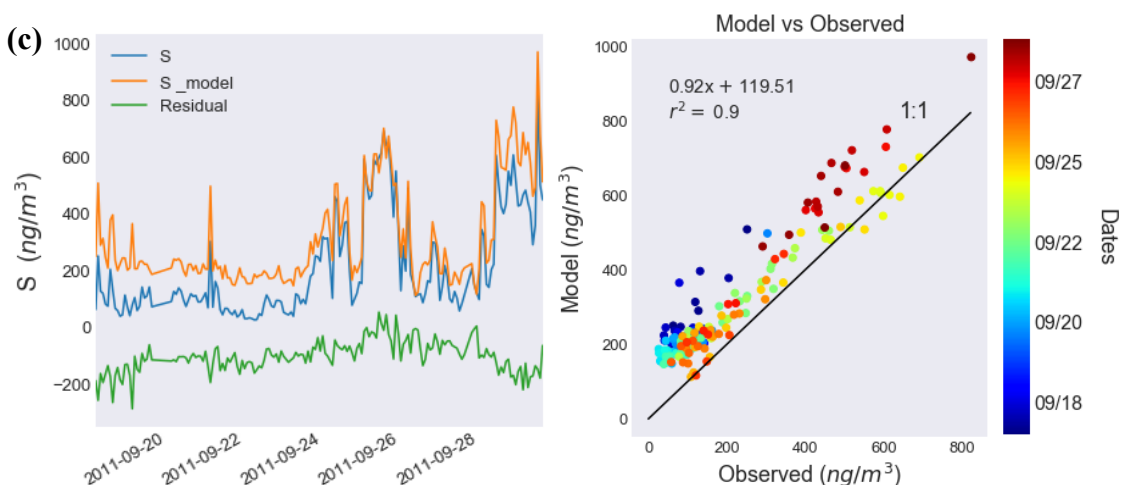
51



52



53



54 **Figure S8. Multiple linear regression time series plots predicting S using tracers K and V**
 55 **in the (a) fine mode, (b) ultrafine mode, and (c) with the addition of Al in the model for**
 56 **the ultrafine mode. The residual is plotted in green, defined as the difference between the**
 57 **actual and modelled concentrations of S. Color bar indicates the time of sampling.**

58 *Multiple linear regression analysis description*

59 Having origins in both oil combustion (Balasubramanian et al., 2003; Han et al., 2006;
60 Santoso et al., 2010) and biomass burning (Artaxo et al., 1998; Han et al., 2006; Reid et al.,
61 2015), S serves as a general indicator combustion (Atwood et al., 2012). Multiple linear
62 regression was used with S as the dependent variable to determine contributions from biomass
63 burning and oil combustion in the fine and ultrafine modes. One key assumption is that
64 variations in S can be attributed to biomass burning and oil combustion, represented by their
65 tracers K and V, respectively.

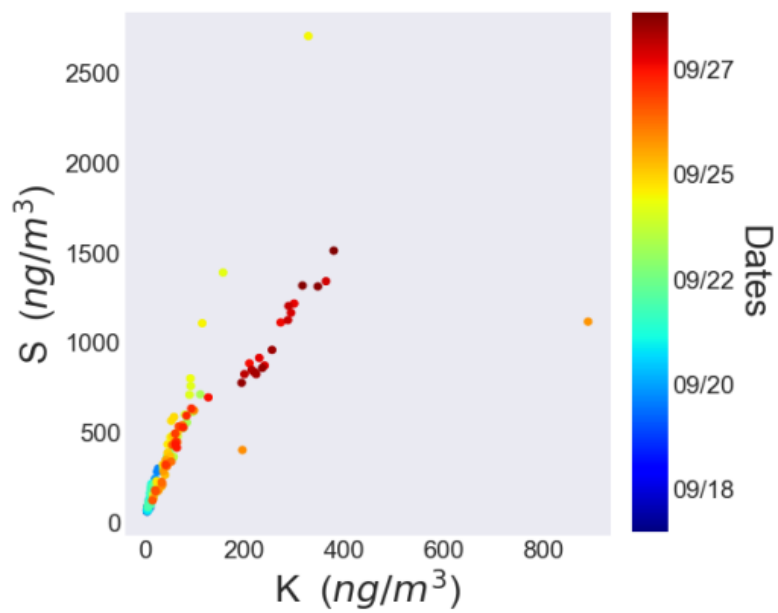
66 Strong correlations, slopes near unity, and low y-intercepts in the linear regression plots
67 of actual and modelled S indicate that K and V are good predictors of S, particularly in the fine
68 mode (Fig. S7a). However, the model underestimates the concentration of ultrafine S between
69 24 to 26 September (Fig. S7b). The underestimation may be due to an additional source of
70 ultrafine S that is independent of biomass burning and oil combustion.

71 To further investigate additional elements that may explain the model's underestimation,
72 residual values between the modelled and actual concentrations of S were used to identify
73 elements that correlated strongly with the residual. In the ultrafine mode, Al was found to
74 correlate strongly with the residual. Upon adding Al to the model, the model was observed to
75 better capture variance in S, specifically between 24 and 26 September (Fig. S7c) which was
76 significantly underestimated when only K and V were included in the model (Fig. S7b). This
77 addition creates a positive discrepancy of the model over the actual concentration of S which
78 indicates source of Al distinct from S in the ultrafine mode. Although the addition of Al
79 improves the model's prediction between 24 and 26 September, we consider K and V generally
80 sufficient predictors of S.

81

82

83



84

85 **Figure S9. Linear regression of S and K in the fine mode (0.34 – 1.15 μm), colored by**
86 **date.**